Article

Not peer-reviewed version

Effect of Corona Treatment Method to Carvacrol Nanocoating Process for Carvacrol/Halloysite-Nanotube/Low-Density-Polyethylene Active Packaging Films Development

Aris E. Giannakas *, Vassilios K Karabagias, Amarildo Ndreka, Aikaterini Dimitrakou, Areti A. Leontiou, Katerina Katerinopoulou, Michael A Karakassides, Charalampos Proestos, Constantinos E Salmas *

Posted Date: 27 May 2024

doi: 10.20944/preprints202405.1704.v1

Keywords: Low density polyethylene; carvacrol; halloysite nanotube; corona treatment; nanocoating; active packaging; control release

Article

Effect of Corona Treatment Method to Carvacrol Nanocoating Process for Carvacrol/ Halloysite-nanotube/Low-Density-Polyethylene Active Packaging Films Development

Aris E. Giannakas [1,*], Vassilios K. Karabagias [1], Amarildo Ndreka [1], Aikaterini Dimitrakou [2], Areti Leontiou [1], Katerina Katerinopoulou [1], Michael A. Karakassides [2], Charalampos Proestos [3] and Constantinos E. Salmas [2,*]

[1] Department of Food Science and Technology, University of Patras, 30100 Agrinio, Greece; vkarampagias@upatras.gr (V.K.K.); amarildondreka5@gmail.com (A.N.); aleontiu@upatras.gr (A.L.); akaterin@upatras.gr (K.K.)

[2] Department of Material Science and Engineering, University of Ioannina, 45110 Ioannina, Greece; a.dimitrakou@uoi.gr (A.D.), mkarakas@uoi.gr (M.A.K.)

[3] Laboratory of Food Chemistry, Department of Chemistry, National and Kapodistrian University of Athens Zografou, 15771 Athens, Greece; harpro@chem.uoa.gr (C.P.)

* Correspondence: agiannakas@upatras.gr (A.E.G.); ksalmas@uoi.gr (C.E.S.)

Abstract: Climate change, increasing global food needs, and decreasing global resources brought a new era to human every-day live with a strong turn to circular economy and sustainability. Food packaging and preservation is an important global sector where enchanced research is carried out. New methods such as active packaging and chemical preservatives replacement are of major interest. Many researchers were published studies about active packaging films, replacement of chemical preservatives with natural originated extracts, and novel incorporation procedures. Sequentially to our and other scientists' previous work, in this paper we present the results of the improvement which was achieved by incorporating the developed nanohybrid of natural-halloysite/carvacrol-extract, the pure natural carvacrol extract and the commonly used low-density-polyethylene. The well known corona-treatment procedure was employed to produced the optimum final film and the results shown that the low-density-polyethylene incorporated with natural-halloysite/carvacrol-extract nanohybrid and coated external with extra carvacrol extract exhibited aproximatelly 100% higher Young-Modulus values, slightly decreased ultimate strength by 20%, and almost stable elonation at break properties. The water-vapor and oxygen barrier increased by 40%. Finally, the antioxidant activity of the corrona-treated film increased by 28% compared to the similar but untreated product because of the lower release rate of the carvacrol.

Keywords: low density polyethylene; carvacrol; halloysite nanotube; corona treatment; nanocoating; active packaging; control release

1. Introduction

In the last few years bioeconomy and sustainability trends are affecting all the scientific fields of research and development. In Food Technology and Food Packaging sector there is a trend of replacing chemical additives and preservatives such as butylated hydroxyanisole (BHA) and butylated hydroxytoluene (BHT) from bioactive compounds such as natural extracts and essential oils (EOs) [1–3]. In this direction EOs have extensively studied as antioxidant and antibacterial agents in active packaging systems [4–6]. EOs are biologically active compounds, which are volatile in nature, safe, environmentally friendly, and have good consumer acceptance as they are categorized as generally recognized as safe (GRAS) by USFDA. EOs such as thyme, clove, cinnamon, tea tree, peppermint, oregano, lemongrass, citronella etc., are plant-derived compounds that exhibit

 doi:10.20944/preprints202405.1704.v1

promising inhibitory action against a broad range of food spoilage microorganisms. In the literature there is a plethora of studies with EOs addition on polymers such as polyethylene (PE), low density polyethylene [7–9], polyethylene tetraphthalate (PET) [10], polystyrene (PS) [11] and biopolymers such as starch, chitosan, gelatin, alginates, poly-lactide acid (PLA) active packaging films [12–20]. In addition, there are many studies with use of EOs active components in active packaging systems such as limonene, eugenol, thymol, cinnamaldehyde and carvacrol [21–28]. Carvacrol (CV) is a phenolic monoterpenoid found in EOs of oregano (Origanum vulgare), thyme (Thymus vulgaris), pepperwort (Lepidium flavum), wild bergamot (Citrus aurantium bergamia), and other plants and is useful for its significant antibacterial, antifungal, antimicrobial, and antioxidant activities. CV and thymol (TO) have the same chemical formula; they are structural isomers. The key difference between carvacrol and thymol is that carvacrol contains a hydroxyl group at the ortho position of the benzene ring whereas thymol contains a hydroxyl group at the meta position of the benzene ring CV antimicrobial activity is higher than that of other volatile compounds present in essential oils due to the presence of the free hydroxyl group, hydrophobicity, and the phenol moiety [29].

In the last decade, many technologies have been employed in incorporating EOs and their derivatives in active food packaging films. Because of EOs' volatile nature, the direct incorporation in the packaging film causes their quick loss so technologies such as the adsorption on nanocarriers, e.g. nanoclays, natural zeolite, activated carbon, and silicas, as well as the electrospinning have been proposed and studied in the literature [30–35]. In addition, antibacterial coatings in packaging films are a rising topic in the field of active packaging materials [36–39]. The development of such antibacterial coatings implies the use of novel surface treatment methods such as chemical surface treatment, UV treatment, corona treatment, and plasma treatment [40]. Among them, Corona treatment can activate polymeric surfaces for adhesion of a variety of functional coatings and it could be potentially explored further in terms of creating special antimicrobial coatings based on natural extract and EOs [41–43].

In recent reports, our research group has developed the technology of incorporating EOs and their components into nanostructures such as nanoclays, natural zeolite, and activated carbon for the development of innovative active packaging films, pads, and coating that succeeds in increasing the shelf life of dairy, fruit, and meat products [44–49]. In this paper, a study for the development of antibacterial nano-coatings of CV on the surface of low-density polyethylene (LDPE) films is reported for the first time. LDPE was chosen as one of the most extensively used packaging materials due to its flexibility and good water barrier properties. As “blank” samples a pure LDPE sample, an LDPE sample reinforced with halloysite nanotube (HNT) nanoclay (LDPE/HNT), and a LDPE sample reinforced with halloysite nanotube (HNT) nanoclay modified with CV (LDPE/CV@HNT) were collected. These three starting materials were surface-modified with a CV nanocoating without treatment and after a corona treatment process. The innovative points of the current study which for the first time reported are (i) the application of CV as nano-coating to develop active packaging materials by using novel packaging technologies such as corona treatment, (ii) the application of CV as nanocoating with corona treatment process not only in pure polymeric matrix such as pure LDPE but also in LDPE/HNT and LDPE/CV@HNT nanocomposite active films, (iii) the comparison study via physicochemical characterization and packaging properties characterization between active packaging materials coated with CV via corona treatment method and active packaging materials coated with CV without corona treatment, (iv) the effect of HNT and CV@HNT nano-reinforcement in the effectiveness of CV nano-coating. The overall study provides new perspectives for the application of processes already used in food packaging such as printing ink technologies and packaging surface activation technologies in the utilization of EOs and their derivatives as antioxidant/antimicrobial nanocoatings of food packaging materials.

 doi:10.20944/preprints202405.1704.v1

2. Materials and Methods

2.1. Materials

Carvacrol (CV) with a CAS no: 499-75-2, halloysite nanotubes (HNT) with a CAS. No. 1332-58-7, LDPE with a CAS no. of 9002-88-4 and extra pure DiPhenyl-1-PicrylHydrazyl (DPPH) with CAS no. of 1898-66-4 were supplied by Sigma-Aldrich (Sigma-Aldrich, St. Louis, MO, USA). Thiobarbituric acid (TBA) pro-analyze was purchased from Merck KGaA 64271 Darmstadt, Germany. Acetone 99% for analysis was supplied from Fisher Scientific, Bishop Meadow Road, Loughborough, LE11 SRG, UK.

2.2. Preparation of CV@HNT Nanohybrid

3 g of HNT were dried at 120 °C under vacuum. Then in the dried HNT approximately 5 ml of CV was added drop by drop and under stirring until a slurry was obtained. The obtained slurry was then stirred overnight since the excess of CV evaporated. The obtained CV@HNT nanohybrid powder was stored for further use.

2.3. Preparation of "Blank" LDPE, LDPE/HNT, and LDPE/CV@HNT Films

The development of LDPE, LDPE/HNT, and LDPE/CV@HNT films was done by employing a Mini Lab twin-screw extruder (Haake Mini Lab II, Thermo Scientific, ANTISEL, S.A., Athens, Greece) operated at 140 °C and 100 rpm for 3 min. For pure LDPE film 5 g of LDPE pellets were blended. For the LDPE/HNT and LDPE/CV@HNT films 4.5 g of LDPE pellets were mixed with 0.5 g of pure HNT and 0.5 g of modified CV@HNT powders to obtain films with 10 wt.% HNT and CV@HNT content correspondingly according to the recent publication [46]. The obtained after the extrusion process pellets were thermomechanical transformed into films (see Figure 1) by using a hydraulic press with heated platens and heat-pressing approximately 1.0 g pellets at 110 °C and a constant pressure of 2 MPa to obtain films with 11 cm diameter and average thickness of 0.06 – 0.12 mm.

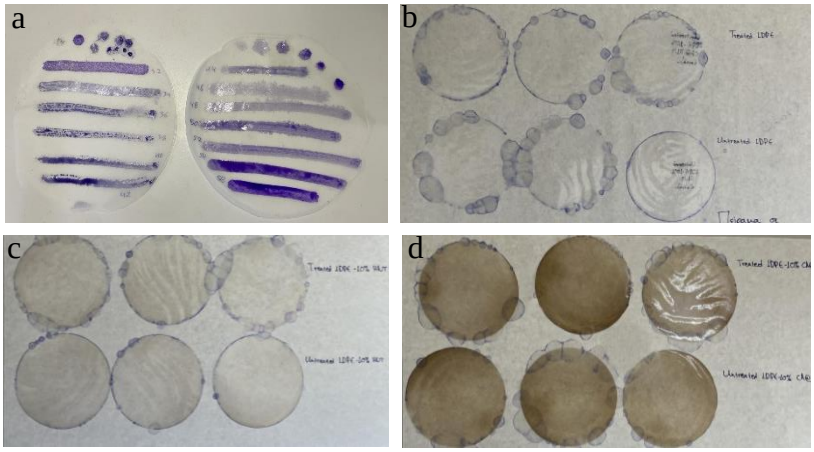

Figure 1. (a) LDPE disk shape (11 cm diameter) films tested with special marker pens for wettability measurements before implying the corona treatment, **(b)** three LDPE films corona treated and coated with CV (upper part) and three LDPE untreated films coated with CV (down part), **(c)** three LDPE/10HNT films corona treated and coated with CV (upper part) and three LDPE/10HNT untreated films coated with CV (down part) and (d) three LDPE/10CV@HNT films corona treated and coated with CV (upper part) and three LDPE/10CV@HNT untreated films coated with CV (down part).

2.4. Preparation of CV Surface-Coated Films

The obtained "blank" LDPE, LDPE/HNT, and LDPE/CV@HNT films were surface coated with CV with two different treatments. One batch of LDPE, LDPE/HNT, and LDPE/CV@HNT films was

 doi:10.20944/preprints202405.1704.v1

surface coated with CV by spreading CV on the external side of the films with a paintbrush. This batch of films is denoted as untreated CV-coated films (see Table 1). A second batch of LDPE, LDPE/HNT, and LDPE/CV@HNT films were firstly corona treated for 30 sec by employing a Handheld Corona Surface Treater Model BD-20V supplied from Electronic-Technic Products (4642 North Ravenswood Ave. Chicago, IL. 60640-4510 U.S.A.). The 30-sec corona treatment time was chosen as the optimum time after the wettability tests carried out in all LDPE, LDPE/HNT, and LDPE/CV@HNT films by using the special marker pens for wettability measurements supplied by Diversified Enterprises, Claremont, NH, USA (see Figure 1). The obtained films after the corona treatment and surface coating with CV were labeled as corona-treated CV-coated films (see Table 1). For each untreated and corona-treated CV-coated film with an 11 cm diameter (see Figure 1) 500 μl of CV was used for the coating process.

Table 1. Code names of all films developed in the current study, amounts of LDPE, HNT, CV@HNT, and CV used, twin extrusion and corona treatment applied conditions.

	LDPE(g)	HNT(g)	CV@HNT(g)	Twin extrusion process time (min) speed (rpm)	Corona treatment -process time (sec)	CV (μl)
LDPE	4.5	-	-	3-100	-	-
LDPE/10HNT	4.5	0.5	-	3-100	-	-
LDPE/10CV@HNT	4.5	-	0.5	3-100	-	-
un-LDPE_CV	4.5	-	-	3-100	-	100
un-LDPE/10HNT_CV	4.5	0.5	-	3-100	-	100
un-LDPE/10CV@HNT_CV	4.5	-	0.5	3-100	-	100
tr-LDPE_CV	4.5	-	-	3-100	30	100
tr-LDPE/10HNT_CV	4.5	0.5	-	3-100	30	100
tr-LDPE/10CV@HNT_CV	4.5	-	0.5	3-100	30	100

2.5. Fourier Transform Infrared (FTIR) Measurements

2.5.1. FTIR Characterization of CV@HNT Nanohybrid and All Obtained Films

All the obtained films as well as pure CV, pure HNT and modified CV@HNT nanohybrid were characterized with FTIR spectroscopy by employing an FT/IR-6000 JASCO Fourier-transform spectrometer (JASCO, Interlab, S.A., Athens, Greece). Typical experimental conditions are set as follows: wavenumber range from 4000 to 400 cm^{-1} and the obtained spectrum was the average of 45 scans at 1 cm^{-1} resolution.

2.5.2. FTIR Study on Corona Treated Films

FTIR spectroscopy was used to investigate possible changes in the chemical composition of corona treated films. For this reason, a batch of the obtained "blank" LDPE, LDPE/HNT and LDPE/CV@HNT films were surface corona treated for 30 sec and immediately measured with FTIR spectroscopy. The obtained FTIR plots compared with the FTIR plots of the LDPE, LDPE/HNT and LDPE/CV@HNT films before the surface treatment.

2.5.3. FTIR Study on Corona-Treated and Untreated CV-Coated Films

FTIR spectroscopy was used as a key method to investigate the possible interaction between CV-coated molecules and chemical groups of all obtained treated and untreated films. For this reason, FTIR plots of un-LDPE_CV, un-LDPE/10HNT_CV, un-LDPE/10CV@HNT_CV films were compared with the FTIR plots of tr-LDPE_CV, tr-LDPE/10HNT_CV, and tr-LDPE/10CV@HNT_CV films.

2.5.4. FTIR Study of CV Release from All Obtained Films

FTIR spectroscopy was used to study the release process of CV from the surface of all obtained films. For such experiments a sample/ of each untreated coated with CV films (un-LDPE_CV, un-

 doi:10.20944/preprints202405.1704.v1

LDPE/10HNT_CV, un-LDPE/10CV@HNT_CV) and a sample of each treated with corona and coated with CV films (tr-LDPE_CV, tr-LDPE/10HNT_CV, and tr-LDPE/10CV@HNT_CV) was kept under ambient conditions and measured for its FTIR spectrum every day for 2 weeks total time.

2.6. Tensile Properties of Films

To investigate the mechanical properties of all the obtained films, tensile measurements were carried out according to the ASTM D638 method and the methodology described in detail recently [46].

2.7. Water/Oxygen Barrier Properties of Obtained Films

2.7.1. Water Vapor Transmission Rate (WVTR) and WATER vapor Diffusion Coefficient (D_{wv})

The WVTR (g/cm².s) for all obtained films, was measured according to the ASTM E96/E 96M-05 method at 38 °C and 95 %RH by using a handmade apparatus. The calculated WVTR values were transformed to D_{wv} values according to the theory and equations described in detail recently [44,50].

2.7.2. Oxygen Transmission Rate Measurements and Oxygen Permeability

Oxygen Transmission Rate (OTR) values (cc O_2/m²/day) for all obtained films, were measured according to the ASTM D 3985 method at 23 °C and 0% RH by employing an oxygen permeation analyzer (O.P.A., 8001, Systech Illinois Instruments Co., Johnsburg, IL, USA). From the measured OTR values the oxygen permeability coefficient values (Pe_{O2}) were calculated according to the theory and equations provided in detail recently [44,50].

2.8. Control Release Kinetics Studies of CV from Obtained Films

For all obtained films the release rate of CV was determined by using a moisture analyzer AXIS AS-60 (AXIS Sp. z o.o. ul. Kartuska 375b, 80-125 Gdańsk) according to the methodology described previously [40]. Approximately, 500 to 700 mg of each film used for each control release experiment. For each film at least three samples were measured. Each film was placed inside the moisture analyzer and its mass was monitored by heating at 70 °C for 1h. By the obtained film mass values (m_t) as a function of time (t) the μg/s CV release rate (R_{CV}) as well as the %wt. CV released content (%RC_{CV}) was determined for each film.

2.9. Antioxidant Activity of Films

For all antioxidant activity experiments a standard solution of [DPPH•] was prepared by desolving 0.0212 g of [DPPH•] free radical in 250 mL of methanol to obtain a 2.16 mM (mmol/L) [DPPH•] free radical methanolic solution. Next, the flask was closed tightly and stirred under dark condition for 12 h to ensure the complete dissolution of [DPPH•] free radical and its pH was measured to ensure its neutrality (7.02± 0.01).

Next a calibration curve of [DPPH•] free radical was made by diluting the 2.16 mM (mmol/L) methanolic solution of [DPPH•] free radical to obtain solutions with concentrations up to 5, 10, 20, 30 and 40 mg/L. Then the absorbance of the obtained diluted methanolic solution of [DPPH•] free radical was measured at 517 nm by employing a SHIMADZU UV-1280 UV/VIS Spectrometer. The calibration curve of absorbance (y) versus concentration (x) of [DPPH•] free radical was expressed by the following equation:

$$y = 0.0388x + 0.015;\ R^2 = 0.9994 \quad (2)$$

2.9.1. Total Antioxidant Activity of Films

The antioxidant activity of all obtained LDPE/xTEO@SBA-15 active films was measured using the 2,2-diphenyl-1-picrylhydrazyl radical (DPPH) assay, as described previously [47,51,52]. Briefly, in 2.8 mL of 30 ppm DPPH ethanolic solution, 0.2 mL of $CH_3COONax3H_2O$ buffer solution, and

Preprints.org (www.preprints.org) | NOT PEER-REVIEWED | Posted: 27 May 2024 doi:10.20944/preprints202405.1704.v1

approximately 2 mg of each LDPE/xTEO@SBA-15 active film was added, and the absorbance at 517 nm was recorded as a function of time every day for 1 weak total time. As a blank sample, the absorbance of 4 mL of 30 ppm DPPH ethanolic solution without the addition of any film was also recorded as a function of time. The % antioxidant activity was calculated by using Equation (3)

$$\%\ DPPH^{\bullet}\ scavenged\ at\ steady\ state\ = \frac{A_0^{517} - A_{sample}^{517}}{A_0^{517}} \times 100 \quad (3)$$

2.8.2. Determination of the Effective Concentration (EC50) of Obtained Films

For the determination of concentration required to obtain 50% antioxidant effect (EC_{50}) of all obtained films 10, 20, 30, 40 and 50 mg of small pieces of each film were placed, in dark vials and three replicates were performed for each sample. Thereafter, 3 mL of [DPPH•] free radical methanolic solution and 2 mL of acetate buffer 100 mM (pH = 7.10) were added in each vial and the absorbance of the reaction mixture was measured at 517 nm after 24h. As a blank sample used a vial where 3 mL of [DPPH•] free radical methanolic solution and 2 mL of acetate buffer was added without the addition of any granule film. The % inhibition of [DPPH•] was calculated using Equation (3).

2.9. Statistical Analysis

All acquired structural, mechanical, antioxidant, and control release kinetic properties were measured experimentaly in triplicate and were subjected to statistical analysis for descriptive statistic values calculations. Furthermore, multiple comparison tests were carried out using Kruskal-Wallis routine to investigate statistical equalities or differences of measn values. Statistical measurements were conducted with a least significance level of $p < 0.05$ using SPSS software (v. 28.0, IBM, Armonk, NY, USA).

3. Results

3.1. FTIR characterization

In the Figure 1 the FTIR plots of pure CV, pure HNT and modified CV@HNT nanohybrid are presented for comparison.

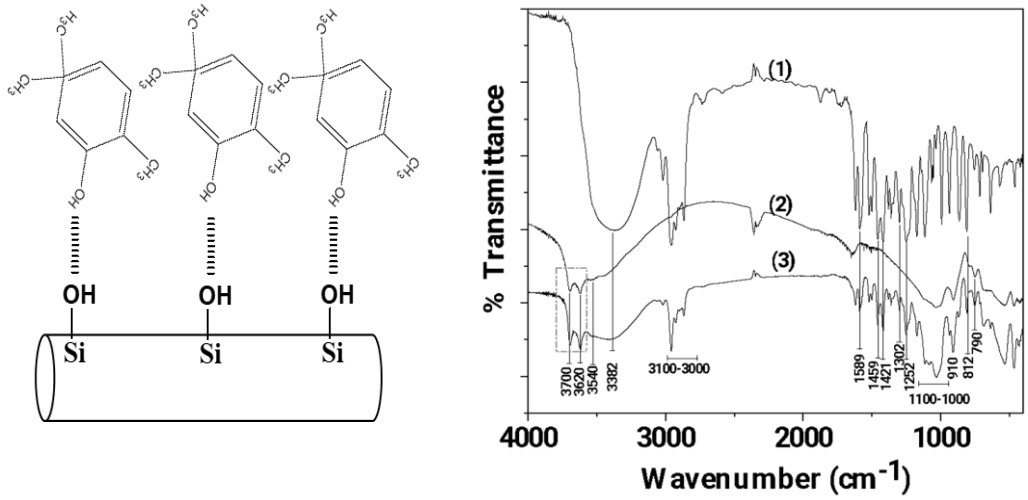

Figure 1. FTIR plots of (1) pure CV, (2) pure HNT and modified (3) CV@HNT nanohybrid.

In the FTIR plot of pure CV (se line (1) in Figure 1) the large broad peak at 3382 cm^{-1} is assigned to the stretching vibration of O-H groups of CV [53,54]. The bands at ~3100–3000 cm^{-1} are corresponded to aromatic and alkenic -CH=CH- stretch vibrations [53,54]. The band at 1589.83 cm^{-1} is assigned to the stretching vibration of C-C bond, at 1459 and at 1421 cm^{-1} are assigned to the

 doi:10.20944/preprints202405.1704.v1

bending vibration of OH groups, at 1302 cm^{-1} is assigned to the isopropyl group $C(CH_3)_2$, at 1252 cm^{-1} is assigned to the stretching vibration of C-O-C group, and at 812 cm^{-1} is assigned to the bending vibration of aromatic C-H bond [53,54].

In the FTIR plot of pure HNT (see the line 2 in Figure 2) the bands at 3700 and 3620 cm^{-1} are assigned to the stretching vibration of hydroxyl groups located in the internal surface of HNT Functionalization of Halloysite Nanotubes by Enlargement and Hydrophobicity for Sustained Release of Analgesic [45,55]. The weak band at 3540 cm^{-1} is assigned to the Si–O–Si (Al) groups [45]. The intense absorption bands in the region of 1100–1000 cm^{-1} and at 790 cm^{-1} are assigned to the Si–O group [55]. The band at 910 cm^{-1} is assigned to the bending vibration of the inner hydroxyl group [55]. The band at 745 cm^{-1} is assigned to the Si–O–Al bonds [45,55].

The FTIR plot of CV@HNT nanohybrid is a mix of both pure CV and pure HNT plots. With a careful glance it is observed that the bands at 3700 and 3620 cm^{-1} which are attributed to internal surface located hydroxyl groups of HNT are increased in the FTIR plot of CV@HNT as compared to the FTIR plot of pure HNT. This reveals an interplay between the hydroxyl groups of CV and hydroxyl groups of HNT located in the external surface as it is illustrated in Figure 1.

In Figure 2 the FTIR plots of pure CV as well as LDPE, LDPE/10HNT and LDPE/10CV@HNT films are shown for comparison.

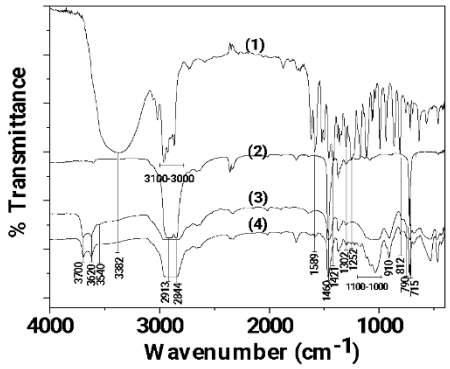

Figure 2. FTIR plots of (1) pure CV as well as (2) LDPE, (3) LDPE/10HNT and (4) LDPE/10CV@HNT films.

In the FTIR plot of pure LDPE film (see plot line (2) in Figure 2) the characteristic peaks of LDPE at 2913, 2844, 1460, and 715 cm^{-1} are observed [56]. Thea peaks at 2913, 2844 cm^{-1} are assigned to the symmetric stretching vibration of $-CH_2$ group of LDPE, while the peaks at 1460 and 715 cm^{-1} to the wagging and rocking vibration of $-CH_2$ group of LDPE correspondingly [57]. In the FTIR plot of LDPE/10HNT film (see plot line (3) in Figure 2) the characteristic bands of HNT at 3700, 3620, 910 and in the range of 1100-1000 cm^{-1} are observed among with the characteristic bands of LDPE. In the FTIR plot of LDPE/10CV@HNT film (see plot line (4) in Figure 2) the characteristic bands of CV at 3382, 1589, 1421, 1302, 1252, 910, 812 and 790 cm^{-1} are observed among with the characteristic bands of LDPE and HNT. No LDPE's peak shift is observed in both LDPE/10HNT an LDPE/10CV@HNT films according to previous similar reports [46,58].

In Figure 3 the FTIR plots of pure LDPE, LDPE/10HNT and LDPE/10CV@HNT untreated (black lines) and corona treated (blue lines) are shown for comparison.

 doi:10.20944/preprints202405.1704.v1

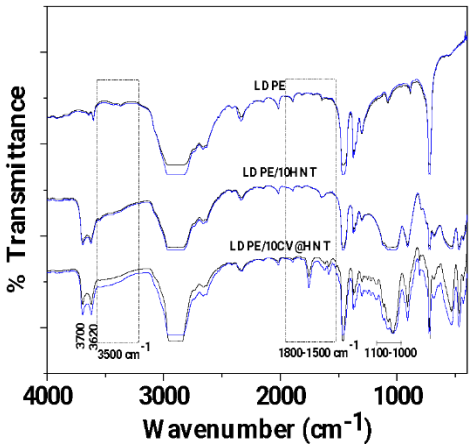

Figure 3. FTIR plots of pure LDPE, LDPE/10HNT and LDPE/10CV@HNT untreated (black lines) and corona treated (blue lines).

With a first glance it is observed that in all cases FTIR plots of all corona treated samples (blue lines) are increased as compared to FTIR plots of all untreated samples (black lines). This is direct evidence of the surface activation achieved by corona treatment in the case of all tested films. According to the literature the increase of bands at 3500 cm^{-1} (see dash dot rectangle region in Figure 3) is evidence of incorporated oxygen-containing functional groups (-OH). The increase of bands in the range 1800–1500 cm^{-1} (see dash dot rectangle region in Figure 3) is an evidence of oxygen species incorporated in carbonylic group (-C=O) while the increase of the absorbance band with a maximum at 1730 cm^{-1} is an evidence of carboxylic acids appeared [59]. With a more careful glance it is observed a higher activation in the case of both LDPE/10HNT and LDPE/10CV@HNT samples as compared to pure LDPE film. Additional activated sites are observed in the case of both LDPE/10HNT and LDPE/10CV@HNT corona treated samples. These are the bands at 3700, 3620 and the bands in the range of 1100 to 1000 cm^{-1} corresponded to surface and inner hydroxyl groups of HNT. In the case of LDPE/10CV@HNT corona treated sample extra active sites are observed in the range of 2000 to 400 cm^{-1} corresponded to CV. Thus, it seems that in the case of LDPE/10HNT and LDPE/10CV@HNT corona treated samples additional oxygen species are incorporated in the hydroxyl groups of HNT for both LDPE/10HNT and LDPE/10CV@HNT samples and in the hydroxyl groups of both HNT and CV molecule for LDPE/10CV@HNT sample. In other words, the incorporation of both HNT and CV@HNT nanohybrid in the LDPE matrix leads to a final matrix with more active sites available for incorporation of oxygen species with corona treatment process.

In Figure 4 the FTIR plots of pure LDPE, un-LDPE_CV and tr-LDPE_CV films are presented for comparison.

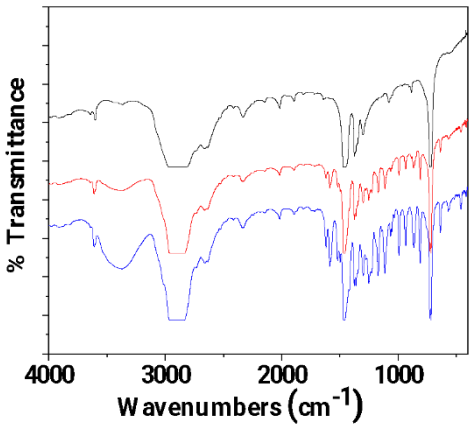

 doi:10.20944/preprints202405.1704.v1

Figure 4. FTIR plots of pure LDPE (black line), un-LDPE_CV (red line) and tr-LDPE_CV (blue line) films.

It is obvious that in FTIR plot of tr-LDPE_CV film the bands corresponded to CV molecules (see the broad band at 3500 cm^{-1} and the bands in the range of 2000-400 cm^{-1}) are higher as compared to the FTIR plot of un-LDPE_CV film. This is a direct proof that corona treatment activates the LDPE surface and results in higher amount of adsorbed CV in the case of tr-LDPE_CV film as compared to the CV adsorbed amount in the case of un-LDPE_CV film.

In Figure 5 the FTIR plots of pure LDPE/10HNT, un-LDPE/10HNT _CV and tr-LDPE/10HNT _CV films are presented for comparison.

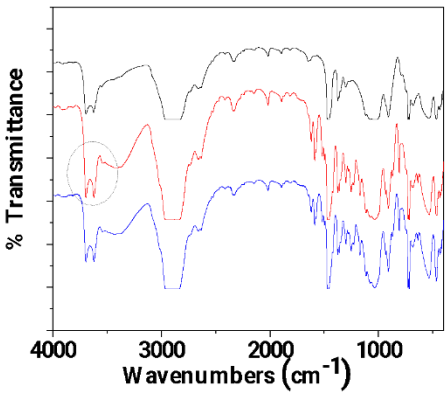

Figure 5. FTIR plots of pure LDPE/10HNT, un-LDPE/10HNT _CV and tr-LDPE/10HNT _CV films.

In Figure 5 it is observed that the bands corresponded to CV molecules (see the broad band at 3500 cm^{-1} and the bands in the range of 2000-400 cm^{-1}) are almost equal for both un-LDPE/10HNT _CV and tr-LDPE/10HNT _CV. This means that both corona treated and untreated LDPE/10HNT films adsorbed almost equal amounts of CV. This result seems controversial at first as it could be expected that corona treatment should led to the adsorption of higher CV amount in the case of tr-LDPE/10HNT _CV as compared to the adsorbed amount of CV in the case of un-LDPE/10HNT _CV film. With a more careful glance in the FTIR plot of un-LDPE/10HNT _CV it is observed that the bands at 3700 and 3620 cm^{-1} (see the region denoted with the gray colored dash dot circle) corresponded to the hydroxyl groups of HNT located in the external surface are much higher as compared to the same bands in the case of FTIR plot of pure LDPE/10HNT film. This activation of HNT's hydroxyl groups suggest a relaxation of this hydroxyl groups with the coated molecules of CV. Thus, it seems that the presence of HNT in LDPE/10HNT film increase the active site where CV molecules can be adsorbed and thus the obtained un-LDPE/10HNT _CV film with coated CV molecules adsorbed equal amounts of CV molecules as compared to the amount of CV molecules adsorbed in the case of corona treated tr-LDPE/10HNT _CV film.

In Figure 6 the FTIR plots of pure LDPE/10CV@HNT, un-LDPE/10CV@HNT _CV and tr-LDPE/10CV@HNT _CV films are presented for comparison.

 doi:10.20944/preprints202405.1704.v1

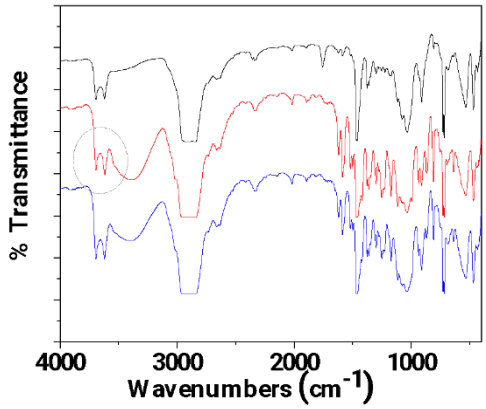

Figure 6. FTIR plots of pure LDPE/10CV@HNT, un-LDPE/10CV@HNT _CV and tr-LDPE/10CV@HNT _CV films.

In Figure 6 it is observed that the bands corresponded to CV molecules (see the broad band at 3500 cm^{-1} and the bands in the range of 2000-400 cm^{-1}) are almost equal for both un-LDPE/10CV@HNT _CV and tr-LDPE/10CV@HNT _CV as in the case of un-LDPE/10HNT _CV and tr-LDPE/10HNT _CV films. Also, the same activation in the bands of HNT's external surface located hydroxyl groups (see the bands at 3700 and 3620 cm^{-1} (denoted with the gray colored dash dot circle) in the FTIR plot of un-LDPE/10CV@HNT _CV film as in the case of un-LDPE/10HNT _CV film it is observed. Thus, it seems that the presence of CV@HNT nanohybrid in LDPE/10CV@HNT film increase the active site where CV molecules can be adsorbed because of the presence of CV molecules inside the LDPE/10CV@HNT film and because of the presence of hydroxyl groups sited in the external surface of HNT. As a result, the obtained un-LDPE/10CV@HNT _CV film with coated CV molecules adsorbed equal amounts of CV molecules as compared to the corona treated tr-LDPE/10CV@HNT _CV film.

In Figure S1 the FTIR plots of untreated and coated with CV films (un-LDPE_CV, un-LDPE/10HNT_CV, un-LDPE/10CV@HNT_CV) and corona treated and coated with CV films (tr-LDPE_CV, tr-LDPE/10HNT_CV, and tr-LDPE/10CV@HNT_CV) on day 1, day 2, day 3, day 4, day 7, day 9, day 11, and day 14 are shown for comparison. For better comparison the same FTIR plots have been zoomed in the range of 1440 to 400 cm^{-1} where the most bands of CV molecules are observed and shown in Figure 7.

 doi:10.20944/preprints202405.1704.v1

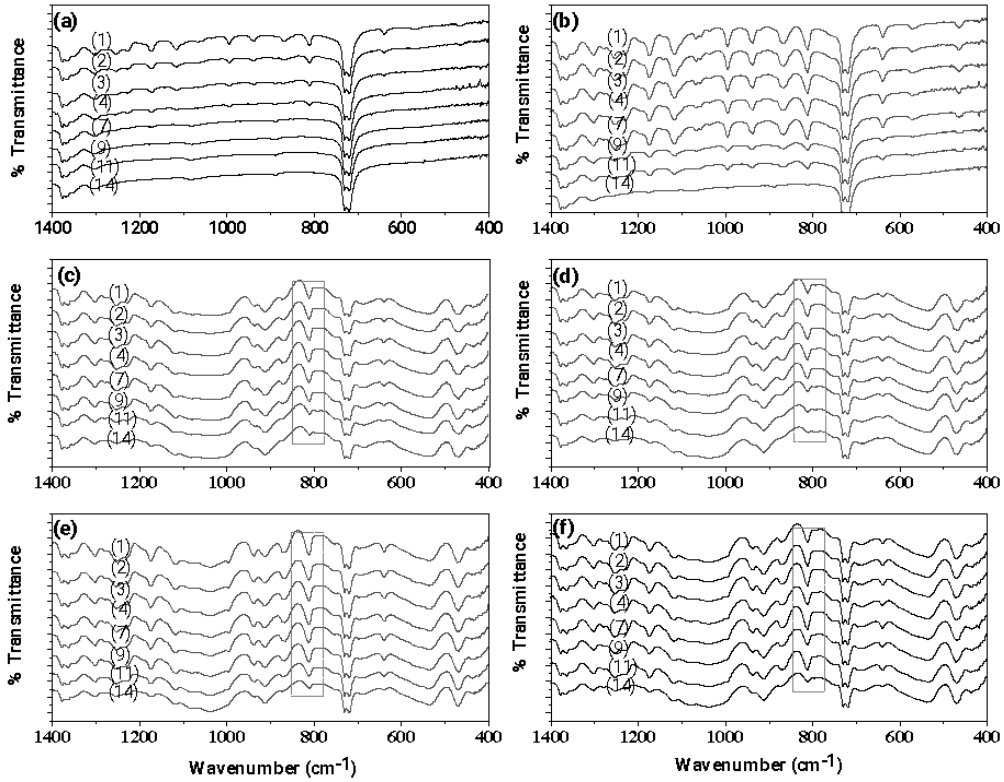

Figure 7. FTIR plots of (left row of graphs): untreated and coated with CV films (a) un-LDPE_CV, (c) un-LDPE/10HNT_CV, (e) un-LDPE/10CV@HNT_CV and of (right row of graphs): corona treated and coated with CV films (b) tr-LDPE_CV, (d) tr-LDPE/10HNT_CV, and (f) tr-LDPE/10CV@HNT_CV on day 1, day 2, day 3, day 4, day 7, day 9, day 11, and day 14.

Comparing the FTIR plots of un-LDPE_CV film (see graph (a) in Figure 7) and tr-LDPE_CV (see graph (b) in Figure 7) it is obvious that in the case of un-LDPE_CV film the CV molecules released quickly and do not detect in the surface of un-LDPE_CV film after the fourth day. On the contrary in the case of tr-LDPE_CV the release of CV molecules is slower, and the CV molecules are detectable in the surface of tr-LDPE_CV since the 11th day. In the case of un-LDPE/10HNT_CV (see graph (c) in Figure 7), tr-LDPE/10HNT_CV (see graph (d) in Figure 7), un-LDPE/10CV@HNT_CV (see graph (e) in Figure 7) and tr-LDPE/10CV@HNT_CV (see graph (f) in Figure 7) films the release of CV molecules is slower and the bands of CV molecules are detectable in the surface of un-LDPE/10HNT_CV, tr-LDPE/10HNT_CV, un-LDPE/10CV@HNT_CV and tr-LDPE/10CV@HNT_CV films since the 14th day (see the denoted with gray dash dot line rectangle band of CV at 812 cm^{-1}). This result is in accordance with the discussion mentioned hereabove where it was suggested that the presence of active sites of HNT in un-LDPE/10HNT_CV film and the presence of active site of both HNT and CV molecules in un-LDPE/10CV@HNT_CV film makes such films able to adsorb equal amounts of CV as the tr-LDPE/10HNT_CV and tr-LDPE/10CV@HNT_CV correspondingly.

3.2. Tensile Properties

For all tested films and their obtained stress-strain curves the Young's Modulus (E), ultimate strength (σ_{uts}) and %elongation at break values were calculated and listed in Table S1. For comparison the same Young's Modulus (E), ultimate strength (σ_{uts}) and %elongation at break values were plotted in column bar diagrams in Figure 8.

Preprints.org (www.preprints.org) | NOT PEER-REVIEWED | Posted: 27 May 2024 doi:10.20944/preprints202405.1704.v1

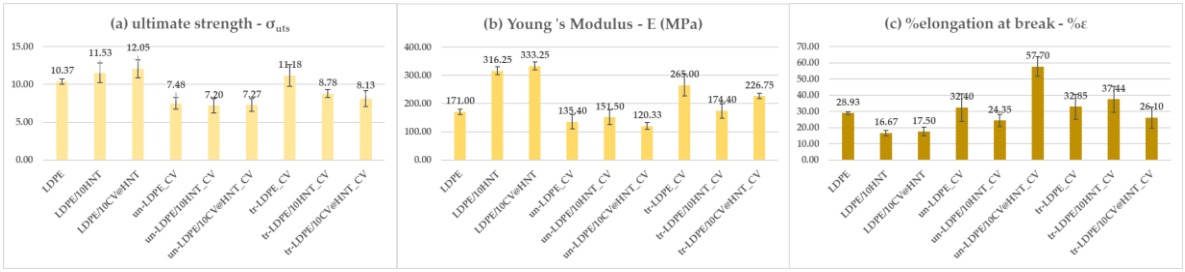

Figure 8. Column bar diagrams of (a) ultimate strength – σ_{uts}, (b) Young's Modulus – E, and (c) %elongation at break values of all tested films.

As it is obtained from the calculated Young's Modulus (E), ultimate strength (σ_{uts}) and %elongation at break values in Table S1 and Figure 8 addition of pure HNT and CV@HNT nanohybrid enhances both stress and ultimate strength and decrease ductility of obtained LDPE/10HNT and LDPE/10CV@HNT films implying the creation of nanocomposite nanostructure in accordance with previous reports [46]. On the other hand, when the surface CV nanocoating it is applied stress and strength values are decreased both in treated and untreated samples as compared to uncoated samples. For un-LDPE_CV and tr-LDPE_CV samples ductility does not significantly change as compared to pure LDPE film while for un-LDPE/10HNT_CV, un-LDPE/10CV@HNT_CV, tr-LDPE/10HNT_CV, and tr-LDPE/10CV@HNT_CV films ductility is significantly decreased as compared to the ductility of LDPE/10HNT and LDPE/10CV@HNT films.

3.3. Water/Oxygen Barrier Properties

In Table S2 the obtained water vapor transmission rate (WVTR), and oxygen transmission rate (OTR) mean values of all tested films are listed for comparison. From these values the water vapor diffusion coefficient (D_{wv}) values and the oxygen permeability (Pe_{O2}) values were calculated and listed also in the Table S2. For comparison the obtained D_{wv} and Pe_{O2} values are also plotted in the column bar diagram in Figure 9.

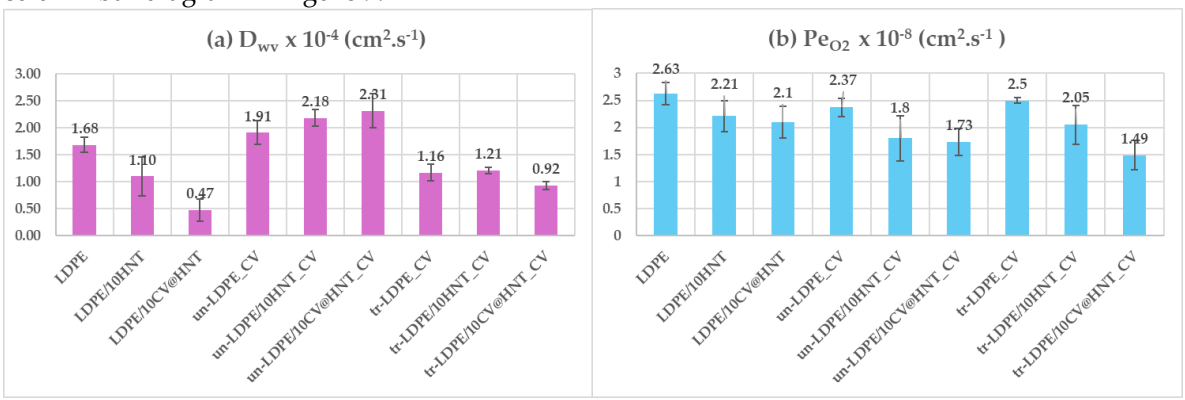

Figure 9. Column bar diagrams of obtained **(a)** D_{wv} and **(b)** Pe_{O2} values for all tested films.

From the water vapor diffusion coefficient (D_{wv}) values plotted in Figure 9(a) it is obtained that addition of both pure HNT and CV@HNT nanohybrid increases the water barrier of obtained LDPE/10HNT and LDP/10CV@HNT nanocomposite films according to previous report [46]. The CV surface nanocoating with or without corona treatment seems to have controversial results in the water barrier properties. The un-LDPE_CV film exhibited no significant difference water barrier as compared to pure LDPE film. The un-LDPE/10HNT_CV and the un-LDPE10/CV@HNT_CV films exhibited lower water barrier properties as compared to the pure LDPE film and much lower water barrier as compared to LDPE/10HNT and LDPE/10CV@HNT films correspondingly. The tr-LDPE_CV, tr-LDPE/10HNT_CV and tr-LDPE/10CV@HNT films exhibited higher water barrier properties than pure LDPE film and lower water barrier than LDPE/10HNT and LDPE/10CV@HNT

 doi:10.20944/preprints202405.1704.v1

films. In addition, all corona treated films exhibited higher water barrier properties than untreated films. This result validates the corona treatment process for applying CV nanocoating on the surface of pure LDPE film and LDPE/10HNT and LDPE/10CV@HNT nanocomposite films. A possible explanation for the superiority of corona treated films against untreated could be the surface bonding of CV molecules on corona treated surface of LDPE film and LDPE/10HNT and LDPE/10CV@HNT nanocomposite films against the naughty or les bonded coating of CV molecules on the untreated surface of LDPE film and LDPE/10HNT and LDPE/10CV@HNT nanocomposite films.

From the P_{eO2} values plotted in Figure 9b it is observed that both corona treated and untreated films do no exhibited significant different values as compared to pure LDPE film as well as LDPE/10HNT and LDPE/10CV@HNT nanocomposite films. Only the film tr-LDPE/10CV@HNT_CV exhibited significant lower P_{eO2} as compared to pure LDPE film as well as LDPE/10HNT and LDPE/10CV@HNT nanocomposite films.

3.4. CV release Kinetics

The CV release rate (R_{CV}) as well as the %wt. CV release content (%RC_{CV}) was calculated for all films and listed in Table S3. The recorded values are also plotted in Figure 10 for comparison.

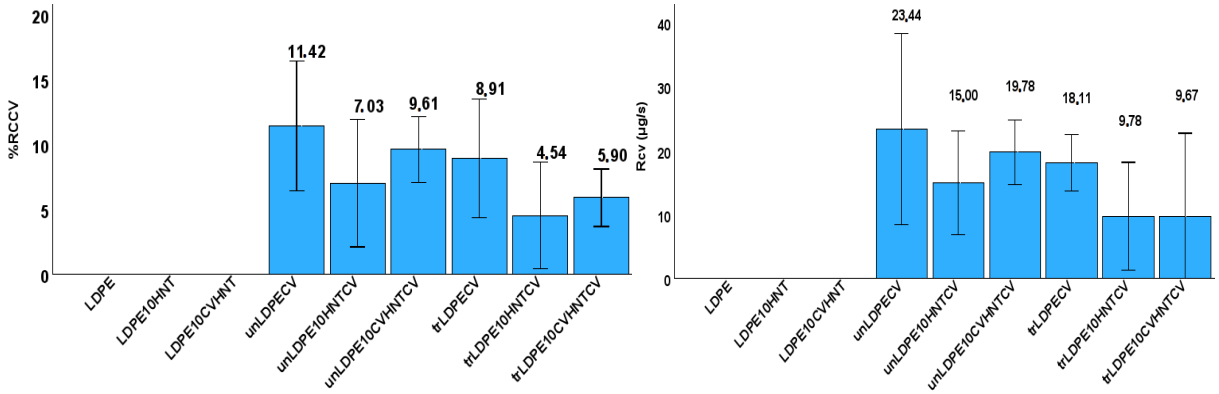

As it is obtained from the values listed in Table S3 all corona treated samples release lower %wt. CV contents with lower release rates as compared to untreated samples. This result combine with the FTIR characterization results discussed hereabove and it is a direct proof that corona treatment leads to a CV surface coating bonded on the surface of the film which is constant and do not release. In addition, from the %RC_{cv} values listed in Table S3 it is evident that the incorporation of HNT nanostructure and CV@HNT nanohybrid in LDPE matrix increased the surface bonding of CV molecules in both corona treated and untreated active films. This result also is in accordance with the FTIR characterization discussion here above where it was shown that the incorporation of both HNT and CV@HNT nanohybrid in the LDPE matrix leads to a final matrix with more active sites available for incorporation of oxygen species with corona treatment process.

3.5. Antioxidant Activity of Films

The calculated total antioxidant activity values of all obtained active films as a function of day are plotted in Figure 11a. The calculated EC_{50} mean values for all obtained active films are plotted in column bar diagram in Figure 11b and listed in Table S4.

 doi:10.20944/preprints202405.1704.v1

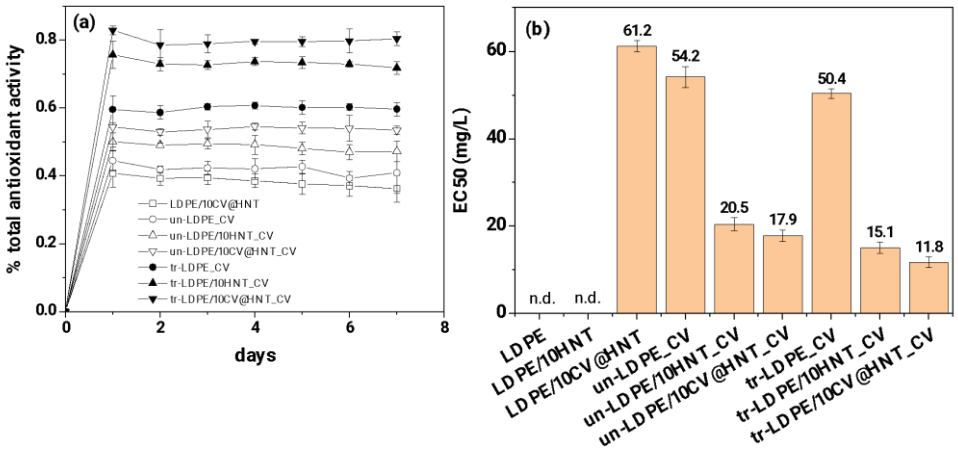

Figure 11. (a) total antioxidant activity of all tested active films as a function of time (days) and **(b)** mean EC_{50} values for all tested active films.

As it is obtained in Figure (a) and Figure (b) both corona treated and untreated CV coated samples obtain higher % total antioxidant activity values and lower EC_{50} values than LDPE/10CV@HNT active film. In addition, all corona treated CV coated samples exhibited higher % total antioxidant activity values and lower EC_{50} values than untreated CV coated samples. This result is in accordance the results of CV release kinetics and show that corona treated films succeed to bond higher amounts of CV which do not release and result in higher antioxidant activity values than untreated CV coated samples where lower amounts of CV molecules are bonded on the surface of the film.

4. Discussion

In this work, a pure LDPE film, a LDPE/10HNT nanocomposite film, and an LDPE/10CV@HNT nanocomposite active film were firstly prepared via an extrusion molding method and used as reference materials to develop CV nanocoatings on their surface. A batch of LDPE, LDPE/10HNT and LDPE/10CV@HNT films were coated with CV on their one site surface without corona treatment to obtain un-LDPE_CV, un-LDPE/10HNT_CV, and un-LDPE/10CV@HNT_CV active films, and another batch of LDPE, LDPE/10HNT and LDPE/10CV@HNT films were firstly surface activated with corona treatment process and secondly coated with CV on their one site surface tr-LDPE_CV, tr-LDPE/10HNT_CV and tr-LDPE/10CV@HNT_CV. FTIR spectroscopy was used as a key method to: (i) characterize CV@HNT nanohybrid and the reference materials LDPE, LDPE/10HNT and LDPE/10CV@HNT, (ii) to study the effect of corona treatment process on the active sites of LDPE, LDPE/10HNT and LDPE/10CV@HNT reference materials, (iii) to study the differences in relaxations between untreated CV coated films and corona treated CV coated films, and (iv) to study the release of CV molecules from the surface of untreated CV coated films and corona treated CV coated films during a two weeks period under abient temperature. As it was shown by FTIR measurements in surface corona treated LDPE, LDPE/10HNT and LDPE/10CV@HNT films the incorporation of both HNT and CV@HNT nanohybrid in the LDPE matrix leads to a final matrix with more active sites available for regeneration of oxygen species with corona treatment process. In addition, FTIR measurament shown that tr-LDPE_CV film adsorbes higher amounts of CV molecules than un-LDPE_CV because of corona treatment activation. This result is in accordance with previous reports [41–43,59,60]. On the other hand un-LDPE/10HNT_CV and un-LDPE/10CV@HNT_CV active films adsorbed equal CV amounts with tr-LDPE/10HNT_CV and tr-LDPE/10CV@HNT_CV active films because of the additional active sites of pure HNT and CV@HNT nanohybrid. These results are for first time reported as it is a first time were such LDPE/10HNT and LDPE/10CV@HNT nanocomposite matrixes corona treated. These reuslts were confirmed by the results of FTIR study on the CV

 doi:10.20944/preprints202405.1704.v1

molecules release from the surface of all obtained CV coated (both treated and untreated) active films. As it was shown CV released faster from the surface of un-LDPE_CV film than the surface of tr-LDPE_CV film while seems to have the same release rate from the surface of un-LDPE/10HNT_CV and un-LDPE/10CV@HNT_CV films as well as from the sueface of tr-LDPE/10HNT_CV and tr-LDPE/10CV@HNT_CV films. To study in more detail the CV molecules release mechanism CV release kinetics experiments were carried out. CV release kinetic experiments were in accordance with FTIR characterizatio results and confirmed that: (i) all corona treated samples release lower %wt. CV contents with lower release rates as compared to untreated samples, (ii) the incorporation of HNT nanostructure and CV@HNT nanohybrid in LDPE matrix increased the surface bonding of CV molecules in both corona treated and untreated active films. Such CV release kinetics experiments results suggest that corona treatment leads to a CV surface coating bonded on the surface of the film which is constant and do not release. The results from CV release kinetics supported by antioxidant activity reuslts where it was shown that all corona treated CV coated films exhibited higher total antioxidant activity and EC50 values than the untreated CV coated films. Overall active films tr-LDPE/10HNT_CV and tr-LDPE/10CV@HNT films are the most promising because they suceed to have a nanocoated CV amount a CV amount ready to release. The un-LDPE/10HNT_CV and un-LDPE/10CV@HNT films also suceed to have a nanocoated CV amount because of CV molecule boanding with extra surface sites created by HNT and CV@HNT nanohybrid but the nanocoated CV amount in the case of un-LDPE/10HNT_CV and un-LDPE/10CV@HNT films is lower than the nanocoated CV amount in the case of tr-LDPE/10HNT_CV and tr-LDPE/10CV@HNT films. These two tr-LDPE/10HNT_CV and tr-LDPE/10CV@HNT films exhibited aslo lower water/oxygen barrier properties than pure LDPE film. Both CV coated corona treated films and CV coated untreated films exhibited lower ultimate strength values than reference materials while their dactility do not statistically significant changed. Overall the tr-LDPE/10CV@HNT active film seems to be the most promising as it is suceed to have an internal deposited amount of CV and a surface nanocoated CV amount. This tr-LDPE/10CV@HNT active film exhibited 45.2% higher water barrier, 43.3% higher oxygen, and 21.1% lower ultimate strength than than pure LDPE film.

5. Conclusions

In this study a novel approach to incorporate EOs and their derivatives, such as CV, in active food packaging materials is presented by developing CV nanocoatings in the surface of pure LDPE film, LDPE/10HNT and LDPE/10CV@HNT nanocomposite films to obtain un-LDPE_CV, un-LDPE/10HNT, un-LDPE/10CV@HNT, and tr-LDPE_CV, tr-LDPE/10HNT, r-LDPE/10CV@HNT CV activated films correspondingly. The development of such CV nanocoatings took place both without pretreatment with the corona process and with pretreatment with the corona process, for comparison. Indeed a novel approach was performed also in the study for the physicochemical characterization and packaging properties characterization of all obtained materials. By targeted FTIR spectroscopy analyses showed that the incorporation of both HNT and CV@HNT nanohybrid in the LDPE matrix leads to a final matrix with more active sites available for the regeneration of oxygen species with the corona treatment process. As a result tr-LDPE_CV film adsorbes higher amounts of CV molecules than un-LDPE_CV because of corona treatment activation while un-LDPE/10HNT_CV and un-LDPE/10CV@HNT_CV active films adsorbed equal CV amounts with tr-LDPE/10HNT_CV and tr-LDPE/10CV@HNT_CV active films because of the additional active sites of pure HNT and CV@HNT nanohybrid. This result also verified by CV release kinetic results where it was shown that in un-LDPE/10HNT_CV, un-LDPE/10CV@HNT_CV, tr-LDPE/10HNT_CV and tr-LDPE/10CV@HNT_CV active films it is created a bonded CV nanolayer which cannot release from the surface of nanocoated films. This bonded CV nanolayer is higher in the case of tr-LDPE/10HNT_CV and tr-LDPE/10CV@HNT_CV activated films than in the case of un-LDPE/10HNT_CV, un-LDPE/10CV@HNT_CV activated films. Overall corona treatment process leads to the optional activated films. All obtained tr-LDPE_CV, tr-LDPE/10HNT_CV, and tr-LDPE/10CV@HNT_CV active films have higher total antioxidant activity and higher EC50 values than un-LDPE_CV, un-LDPE/10HNT_CV and un-LDPE/10CV@HNT_CV active films. The most promising active films

 doi:10.20944/preprints202405.1704.v1

seems to be the tr-LDPE/10CV@HNT_CV active film which exhibited 45.2% higher water barrier, and 43.3% higher oxygen than pure LDPE film. This active film could be potentially be used as a novel active film with a CV amount incorporated inside the polymer matrix slowly released and onother CV amount nanocoated and partially bonded on its one side surface.

Supplementary Materials: The following supporting information can be downloaded at the website of this paper posted on Preprints.org, Figure S1: FTIR plots of (left row of graphs): untreated and coated with CV films (a) un-LDPE_CV, (c) un-LDPE/10HNT_CV, (e) un-LDPE/10CV@HNT_CV and of (right row of graphs): corona treated and coated with CV films (b) tr-LDPE_CV, (d) tr-LDPE/10HNT_CV, and (f) tr-LDPE/10CV@HNT_CV on day 1, day 2, day 3, day 4, day 7, day 9, day 11, and day 14; Table S1: Calculated Young's Modulus (E), ultimate strength (σ_{uts}) and %elongation at break mean values among with the standard deviation values and statistical analysis results; Table S2: Calculated WVTR, D_{wv}, O.T.R. and Pe_{O2} mean values among with the standard deviation values and statistical analysis results for all tested films. Table S3: Calculated %wt. CV release content (%RC_{CV}) as well as the CV release rate (RR_{CV}) mean values for all corona treated and untreated active films. Table S4: Calculated EC_{50} mean values among with standard deviation values and statistical analysis results for all tested films.

Author Contributions: Conceptualization, A.E.G., C. P. and C.E.S; Data curation, V.K.K., A.D., A.L., M.A.K. and C.P.; Formal analysis, A.E.G., A.L., K.K., C.P. and C.E.S.; Investigation, A.E.G., V.K.K., A.N., A.D., A.L., K.K., M.A.K., C.P. and C.E.S.; Methodology, A.E.G., M.A.K., C.P. and C.E.S.; Project administration, A.E.G. and C.E.S.; Resources, A.E.G. and C.E.S.; Software, C.E.S.; Supervision, A.E.G. and C.E.S.; Validation, A.E.G. and C.E.S.; Visualization, A.E.G. and C.E.S.; Writing – original draft, A.E.G. and C.E.S.; Writing – review & editing, A.E.G. and C.E.S. All authors have read and agreed to the published version of the manuscript.

Funding: This research was no funded.

Data Availability Statement: The datasets generated for this study are available on request to the corresponding author.

Conflicts of Interest: The authors declare no conflict of interest.

References

1. Scarano, P.; Sciarrillo, R.; Tartaglia, M.; Zuzolo, D.; Guarino, C. Circular Economy and Secondary Raw Materials from Fruits as Sustainable Source for Recovery and Reuse. A Review. *Trends in Food Science & Technology* **2022**, *122*, 157–170, doi:10.1016/j.tifs.2022.02.003.
2. Plant Extracts-Based Food Packaging Films - Natural Materials for Food Packaging Application - Wiley Online Library Available online: https://onlinelibrary.wiley.com/doi/10.1002/9783527837304.ch2 (accessed on 26 July 2023).
3. Hamam, M.; Chinnici, G.; Di Vita, G.; Pappalardo, G.; Pecorino, B.; Maesano, G.; D'Amico, M. Circular Economy Models in Agro-Food Systems: A Review. *Sustainability* **2021**, *13*, 3453, doi:10.3390/su13063453.
4. Carpena, M.; Nuñez-Estevez, B.; Soria-Lopez, A.; Garcia-Oliveira, P.; Prieto, M.A. Essential Oils and Their Application on Active Packaging Systems: A Review. *Resources* **2021**, *10*, 7, doi:10.3390/resources10010007.
5. Chacha, J.S.; Ofoedu, C.E.; Xiao, K. Essential Oil-Based Active Polymer-Based Packaging System: A Review of Its Effect on the Antimicrobial, Antioxidant, and Sensory Properties of Beef and Chicken Meat. *Journal of Food Processing and Preservation* **2022**, *46*, e16933, doi:10.1111/jfpp.16933.
6. Use of Essential Oils in Bioactive Edible Coatings: A Review | SpringerLink Available online: https://link.springer.com/article/10.1007/s12393-010-9031-3 (accessed on 8 August 2019).
7. Busolo, M.A.; Lagaron, J.M. Antioxidant Polyethylene Films Based on a Resveratrol Containing Clay of Interest in Food Packaging Applications. *Food Packaging and Shelf Life* **2015**, *6*, 30–41, doi:10.1016/j.fpsl.2015.08.004.
8. Coelho, L.B.; Geraldine, R.M.; Silveira, M.F.A.; Souza, A.R.M. de; Torres, M.C.L.; Gonçalves, M.Á.B. Characterization of Films of Low Density Polyethylene Incorporated with Oregano Essential Oil. *Research, Society and Development* **2020**, *9*, e3849108722–e3849108722, doi:10.33448/rsd-v9i10.8722.
9. de Araújo, L.O.; Anaya, K.; Pergher, S.B.C. Synthesis of Antimicrobial Films Based on Low-Density Polyethylene (LDPE) and Zeolite A Containing Silver. *Coatings* **2019**, *9*, 786, doi:10.3390/coatings9120786.
10. Farghal, H.H.; Karabagias, I.; El Sayed, M.; Kontominas, M.G. Determination of Antioxidant Activity of Surface-Treated PET Films Coated with Rosemary and Clove Extracts. *Packaging Technology and Science* **2017**, *30*, 799–808, doi:10.1002/pts.2335.
11. Giannakas, A.E.; Salmas, C.E.; Karydis-Messinis, A.; Moschovas, D.; Kollia, E.; Tsigkou, V.; Proestos, C.; Avgeropoulos, A.; Zafeiropoulos, N.E. Nanoclay and Polystyrene Type Efficiency on the Development of Polystyrene/Montmorillonite/Oregano Oil Antioxidant Active Packaging Nanocomposite Films. *Applied Sciences* **2021**, *11*, 9364, doi:10.3390/app11209364.

12. Aitboulahsen, M.; El Galiou, O.; Laglaoui, A.; Bakkali, M.; Hassani Zerrouk, M. Effect of Plasticizer Type and Essential Oils on Mechanical, Physicochemical, and Antimicrobial Characteristics of Gelatin, Starch, and Pectin-Based Films. *Journal of Food Processing and Preservation* **2020**, *44*, e14480, doi:10.1111/jfpp.14480.
13. Souza, A.G.; Ferreira, R.R.; Paula, L.C.; Mitra, S.K.; Rosa, D.S. Starch-Based Films Enriched with Nanocellulose-Stabilized Pickering Emulsions Containing Different Essential Oils for Possible Applications in Food Packaging. *Food Packaging and Shelf Life* **2021**, *27*, 100615, doi:10.1016/j.fpsl.2020.100615.
14. Abdollahi, M.; Rezaei, M.; Farzi, G. A Novel Active Bionanocomposite Film Incorporating Rosemary Essential Oil and Nanoclay into Chitosan. *Journal of Food Engineering* **2012**, *111*, 343–350, doi:10.1016/j.jfoodeng.2012.02.012.
15. Almeida, R.R.; Silva Damasceno, E.T.; de Carvalho, S.Y.B.; de Carvalho, G.S.G.; Gontijo, L.A.P.; de Lima Guimarães, L.G. Chitosan Nanogels Condensed to Ferulic Acid for the Essential Oil of Lippia Origanoides Kunth Encapsulation. *Carbohydrate Polymers* **2018**, *188*, 268–275, doi:10.1016/j.carbpol.2018.01.103.
16. Hasani, S.; Ojagh, S.M.; Ghorbani, M. Nanoencapsulation of Lemon Essential Oil in Chitosan-Hicap System. Part 1: Study on Its Physical and Structural Characteristics. *International Journal of Biological Macromolecules* **2018**, *115*, 143–151, doi:10.1016/j.ijbiomac.2018.04.038.
17. Jiang, J.; Watowita, P.S.M.S.L.; Chen, R.; Shi, Y.; Geng, J.-T.; Takahashi, K.; Li, L.; Osako, K. Multilayer Gelatin/Myofibrillar Films Containing Clove Essential Oil: Properties, Protein-Phenolic Interactions, and Migration of Active Compounds. *Food Packaging and Shelf Life* **2022**, *32*, 100842, doi:10.1016/j.fpsl.2022.100842.
18. Fiore, A.; Park, S.; Volpe, S.; Torrieri, E.; Masi, P. Active Packaging Based on PLA and Chitosan-Caseinate Enriched Rosemary Essential Oil Coating for Fresh Minced Chicken Breast Application. *Food Packaging and Shelf Life* **2021**, *29*, 100708, doi:10.1016/j.fpsl.2021.100708.
19. Wongphan, P.; Nampanya, P.; Chakpha, W.; Promhuad, K.; Laorenza, Y.; Leelaphiwat, P.; Bumbudsanpharoke, N.; Sodsai, J.; Lorenzo, J.M.; Harnkarnsujarit, N. Lesser Galangal (Alpinia Officinarum Hance) Essential Oil Incorporated Biodegradable PLA/PBS Films as Shelf-Life Extension Packaging of Cooked Rice. *Food Packaging and Shelf Life* **2023**, *37*, 101077, doi:10.1016/j.fpsl.2023.101077.
20. Louis, E.; Villalobos-Carvajal, R.; Reyes-Parra, J.; Jara-Quijada, E.; Ruiz, C.; Andrades, P.; Gacitúa, J.; Beldarraín-Iznaga, T. Preservation of Mushrooms (Agaricus Bisporus) by an Alginate-Based-Coating Containing a Cinnamaldehyde Essential Oil Nanoemulsion. *Food Packaging and Shelf Life* **2021**, *28*, 100662, doi:10.1016/j.fpsl.2021.100662.
21. Arrieta, M.P.; López, J.; Ferrándiz, S.; Peltzer, M.A. Characterization of PLA-Limonene Blends for Food Packaging Applications. *Polymer Testing* **2013**, *32*, 760–768, doi:10.1016/j.polymertesting.2013.03.016.
22. Darvish, M.; Ajji, A. Synergistic Antimicrobial Activities of Limonene with Mineral Carriers in LDPE Films for Active Packaging Application. *Science Journal of Chemistry* **2022**, *10*, 32, doi:10.11648/j.sjc.20221002.11.
23. Huang, X.; Ge, X.; Zhou, L.; Wang, Y. Eugenol Embedded Zein and Poly(Lactic Acid) Film as Active Food Packaging: Formation, Characterization, and Antimicrobial Effects. *Food Chemistry* **2022**, *384*, 132482, doi:10.1016/j.foodchem.2022.132482.
24. Srisa, A.; Harnkarnsujarit, N. Antifungal Films from Trans-Cinnamaldehyde Incorporated Poly(Lactic Acid) and Poly(Butylene Adipate-Co-Terephthalate) for Bread Packaging. *Food Chemistry* **2020**, *333*, 127537, doi:10.1016/j.foodchem.2020.127537.
25. Gámez, E.; Elizondo-Castillo, H.; Tascon, J.; García-Salinas, S.; Navascues, N.; Mendoza, G.; Arruebo, M.; Irusta, S. Antibacterial Effect of Thymol Loaded SBA-15 Nanorods Incorporated in PCL Electrospun Fibers. *Nanomaterials (Basel)* **2020**, *10*, 616, doi:10.3390/nano10040616.
26. Ochoa-Velasco, C.E.; Pérez-Pérez, J.C.; Varillas-Torres, J.M.; Navarro-Cruz, A.R.; Hernández-Carranza, P.; Munguía-Pérez, R.; Cid-Pérez, T.S.; Avila-Sosa, R. Starch Edible Films/Coatings Added with Carvacrol and Thymol: In Vitro and In Vivo Evaluation against Colletotrichum Gloeosporioides. *Foods* **2021**, *10*, 175, doi:10.3390/foods10010175.
27. Pei, R.S.; Zhou, F.; Ji, B.P.; Xu, J. Evaluation of Combined Antibacterial Effects of Eugenol, Cinnamaldehyde, Thymol, and Carvacrol against E. Coli with an Improved Method. *Journal of Food Science* **2009**, *74*, 379–383, doi:10.1111/j.1750-3841.2009.01287.x.
28. Babayev, A.; Spasojević, L.; Škrbić, J.; Bučko, S.; Kocić-Tanackov, S.; Bulut, S.; Fraj, J.; Petrović, L.; Milinković Budinčić, J.; Sharipova, A.; et al. Antimicrobial Pseudolatex Zein Films with Encapsulated Carvacrol for Sustainable Food Packaging. *Food Packaging and Shelf Life* **2023**, *37*, 101076, doi:10.1016/j.fpsl.2023.101076.
29. Sharifi-Rad, M.; Varoni, E.M.; Iriti, M.; Martorell, M.; Setzer, W.N.; Del Mar Contreras, M.; Salehi, B.; Soltani-Nejad, A.; Rajabi, S.; Tajbakhsh, M.; et al. Carvacrol and Human Health: A Comprehensive Review. *Phytother Res* **2018**, *32*, 1675–1687, doi:10.1002/ptr.6103.
30. Li, Q.; Ren, T.; Perkins, P.; Hu, X.; Wang, X. Applications of Halloysite Nanotubes in Food Packaging for Improving Film Performance and Food Preservation. *Food Control* **2021**, *124*, 107876, doi:10.1016/j.foodcont.2021.107876.

31. de Oliveira, L.H.; Trigueiro, P.; Souza, J.S.N.; de Carvalho, M.S.; Osajima, J.A.; da Silva-Filho, E.C.; Fonseca, M.G. Montmorillonite with Essential Oils as Antimicrobial Agents, Packaging, Repellents, and Insecticides: An Overview. *Colloids and Surfaces B: Biointerfaces* **2022**, *209*, 112186, doi:10.1016/j.colsurfb.2021.112186.
32. Mitura, K.; Kornacka, J.; Kopczyńska, E.; Kalisz, J.; Czerwińska, E.; Affeltowicz, M.; Kaczorowski, W.; Kolesińska, B.; Frączyk, J.; Bakalova, T.; et al. Active Carbon-Based Nanomaterials in Food Packaging. *Coatings* **2021**, *11*, 161, doi:10.3390/coatings11020161.
33. Villa, C.C.; Valencia, G.A.; López Córdoba, A.; Ortega-Toro, R.; Ahmed, S.; Gutiérrez, T.J. Zeolites for Food Applications: A Review. *Food Bioscience* **2022**, *46*, 101577, doi:10.1016/j.fbio.2022.101577.
34. Videira-Quintela, D.; Martin, O.; Montalvo, G. Emerging Opportunities of Silica-Based Materials within the Food Industry. *Microchemical Journal* **2021**, *167*, 106318, doi:10.1016/j.microc.2021.106318.
35. Kurd, F.; Fathi, M.; Shekarchizadeh, H. Basil Seed Mucilage as a New Source for Electrospinning: Production and Physicochemical Characterization. *International Journal of Biological Macromolecules* **2017**, *95*, 689–695, doi:10.1016/j.ijbiomac.2016.11.116.
36. Suppakul, P.; Miltz, J.; Sonneveld, K.; Bigger, S. w. Active Packaging Technologies with an Emphasis on Antimicrobial Packaging and Its Applications. *Journal of Food Science* **2003**, *68*, 408–420, doi:10.1111/j.1365-2621.2003.tb05687.x.
37. Andrade, M.A.; Barbosa, C.H.; Souza, V.G.L.; Coelhoso, I.M.; Reboleira, J.; Bernardino, S.; Ganhão, R.; Mendes, S.; Fernando, A.L.; Vilarinho, F.; et al. Novel Active Food Packaging Films Based on Whey Protein Incorporated with Seaweed Extract: Development, Characterization, and Application in Fresh Poultry Meat. *Coatings* **2021**, *11*, 229, doi:10.3390/coatings11020229.
38. Gaikwad, K.K.; Singh, S.; Lee, Y.S. A Pyrogallol-Coated Modified LDPE Film as an Oxygen Scavenging Film for Active Packaging Materials. *Progress in Organic Coatings* **2017**, *111*, 186–195, doi:10.1016/j.porgcoat.2017.05.016.
39. Fu, Y.; Dudley, E.G. Antimicrobial-Coated Films as Food Packaging: A Review. *Comprehensive Reviews in Food Science and Food Safety* **2021**, *20*, 3404–3437, doi:10.1111/1541-4337.12769.
40. Tyuftin, A.A.; Kerry, J.P. Review of Surface Treatment Methods for Polyamide Films for Potential Application as Smart Packaging Materials: Surface Structure, Antimicrobial and Spectral Properties. *Food Packaging and Shelf Life* **2020**, *24*, 100475, doi:10.1016/j.fpsl.2020.100475.
41. Louzi, V.C.; Campos, J.S. de C. Corona Treatment Applied to Synthetic Polymeric Monofilaments (PP, PET, and PA-6). *Surfaces and Interfaces* **2019**, *14*, 98–107, doi:10.1016/j.surfin.2018.12.005.
42. Dai, L.; Xu, D. Polyethylene Surface Enhancement by Corona and Chemical Co-Treatment. *Tetrahedron Letters* **2019**, *60*, 1005–1010, doi:10.1016/j.tetlet.2019.03.013.
43. Božović, A.; Tomašević, K.; Benbettaieb, N.; Debeaufort, F. Influence of Surface Corona Discharge Process on Functional and Antioxidant Properties of Bio-Active Coating Applied onto PLA Films. *Antioxidants* **2023**, *12*, 859, doi:10.3390/antiox12040859.
44. Giannakas, A.E.; Salmas, C.E.; Moschovas, D.; Zaharioudakis, K.; Georgopoulos, S.; Asimakopoulos, G.; Aktypis, A.; Proestos, C.; Karakassides, A.; Avgeropoulos, A.; et al. The Increase of Soft Cheese Shelf-Life Packaged with Edible Films Based on Novel Hybrid Nanostructures. *Gels* **2022**, *8*, 539, doi:10.3390/gels8090539.
45. Constantinos E. Salmas; Aris E. Giannakas; Dimitrios Moschovas; Eleni Kollia; Stsvros Georgopoulos; Christina Gioti; Areti Leontiou; Apostolos Avgeropoulos; Anna Kopsacheili; Learda Avdulai; et al. Kiwi Fruits Preservation Using Novel Edible Active Coatings Based on Rich in Thymol Halloysite Nanostructures and Chitosan/Polyvinyl Alcohol Gels. *Gels Bioactive Gel Films and Coatings Applied in Active Food Packaging*.
46. Giannakas, A.E.; Salmas, C.E.; Moschovas, D.; Karabagias, V.K.; Karabagias, I.K.; Baikousi, M.; Georgopoulos, S.; Leontiou, A.; Katerinopoulou, K.; Zafeiropoulos, N.E.; et al. Development, Characterization, and Evaluation as Food Active Packaging of Low-Density-Polyethylene-Based Films Incorporated with Rich in Thymol Halloysite Nanohybrid for Fresh "Scaloppini" Type Pork Meat Fillets Preservation. *Polymers* **2023**, *15*, 282, doi:10.3390/polym15020282.
47. Giannakas, A.E.; Karabagias, V.K.; Moschovas, D.; Leontiou, A.; Karabagias, I.K.; Georgopoulos, S.; Karydis-Messinis, A.; Zaharioudakis, K.; Andritsos, N.; Kehayias, G.; et al. Thymol@activated Carbon Nanohybrid for Low-Density Polyethylene-Based Active Packaging Films for Pork Fillets' Shelf-Life Extension. *Foods* **2023**, *12*, 2590, doi:10.3390/foods12132590.
48. Salmas, C.E.; Kollia, E.; Avdylaj, L.; Kopsacheili, A.; Zaharioudakis, K.; Georgopoulos, S.; Leontiou, A.; Katerinopoulou, K.; Kehayias, G.; Karakassides, A.; et al. Thymol@Natural Zeolite Nanohybrids for Chitosan/Poly-Vinyl-Alcohol Based Hydrogels Applied As Active Pads for Strawberries Preservation 2023.
49. Salmas, C.E.; Giannakas, A.E.; Karabagias, V.K.; Moschovas, D.; Karabagias, I.K.; Gioti, C.; Georgopoulos, S.; Leontiou, A.; Kehayias, G.; Avgeropoulos, A.; et al. Development and Evaluation of a Novel-Thymol@Natural-Zeolite/Low-Density-Polyethylene Active Packaging Film: Applications for Pork Fillets Preservation. *Antioxidants* **2023**, *12*, 523, doi:10.3390/antiox12020523.

50. Salmas, C.E.; Giannakas, A.E.; Baikousi, M.; Kollia, E.; Tsigkou, V.; Proestos, C. Effect of Copper and Titanium-Exchanged Montmorillonite Nanostructures on the Packaging Performance of Chitosan/Poly-Vinyl-Alcohol-Based Active Packaging Nanocomposite Films. *Foods* **2021**, *10*, 3038, doi:10.3390/foods10123038.
51. Brand-Williams, W.; Cuvelier, M.E.; Berset, C. Use of a Free Radical Method to Evaluate Antioxidant Activity. *LWT - Food Science and Technology* **1995**, *28*, 25–30, doi:10.1016/S0023-6438(95)80008-5.
52. Karabagias, I.K.; Maia, M.; Karabagias, V.K.; Gatzias, I.; Badeka, A.V. Characterization of Eucalyptus, Chestnut and Heather Honeys from Portugal Using Multi-Parameter Analysis and Chemo-Calculus. *Foods* **2018**, *7*, 194, doi:10.3390/foods7120194.
53. Tariq Waece Sadeq; Fouad Hussein Kamel; Karzan Omer Qader A Novel Preparation of Thyme Cream as Superficial Antimicrobial Treatment. *Journal of International Pharmaceutical Research* **2019**, *46*, 373–381.
54. Valderrama, A.C.S.; De, G.C.R. Traceability of Active Compounds of Essential Oils in Antimicrobial Food Packaging Using a Chemometric Method by ATR-FTIR. *American Journal of Analytical Chemistry* **2017**, *8*, 726–741, doi:10.4236/ajac.2017.811053.
55. Li, H.; Zhu, X.; Zhou, H.; Zhong, S. Functionalization of Halloysite Nanotubes by Enlargement and Hydrophobicity for Sustained Release of Analgesic. *Colloids and Surfaces A: Physicochemical and Engineering Aspects* **2015**, *487*, 154–161, doi:10.1016/j.colsurfa.2015.09.062.
56. Martínez-Camacho, A.P.; Cortez-Rocha, M.O.; Graciano-Verdugo, A.Z.; Rodríguez-Félix, F.; Castillo-Ortega, M.M.; Burgos-Hernández, A.; Ezquerra-Brauer, J.M.; Plascencia-Jatomea, M. Extruded Films of Blended Chitosan, Low Density Polyethylene and Ethylene Acrylic Acid. *Carbohydr Polym* **2013**, *91*, 666–674, doi:10.1016/j.carbpol.2012.08.076.
57. Giannakas, A.; Salmas, C.; Leontiou, A.; Tsimogiannis, D.; Oreopoulou, A.; Braouhli, J. Novel LDPE/Chitosan Rosemary and Melissa Extract Nanostructured Active Packaging Films. *Nanomaterials* **2019**, *9*, 1105, doi:10.3390/nano9081105.
58. Giannakas, A.E.; Salmas, C.E.; Leontiou, A.; Baikousi, M.; Moschovas, D.; Asimakopoulos, G.; Zafeiropoulos, N.E.; Avgeropoulos, A. Synthesis of a Novel Chitosan/Basil Oil Blend and Development of Novel Low Density Poly Ethylene/Chitosan/Basil Oil Active Packaging Films Following a Melt-Extrusion Process for Enhancing Chicken Breast Fillets Shelf-Life. *Molecules* **2021**, *26*, 1585, doi:10.3390/molecules26061585.
59. Munteanu, B.S.; Sacarescu, L.; Vasiliu, A.-L.; Hitruc, G.E.; Pricope, G.M.; Sivertsvik, M.; Rosnes, J.T.; Vasile, C. Antioxidant/Antibacterial Electrospun Nanocoatings Applied onto PLA Films. *Materials* **2018**, *11*, 1973, doi:10.3390/ma11101973.
60. Cox, H.J.; Sharples, G.J.; Badyal, J.P.S. Tea–Essential Oil–Metal Hybrid Nanocoatings for Bacterial and Viral Inactivation. *ACS Appl. Nano Mater.* **2021**, *4*, 12619–12628, doi:10.1021/acsanm.1c03151.